DFT Investigation of Alkoxide vs Alkylammonium Formation in Amine-Substituted Zeolites

David Lesthaeghe,[†] Veronique Van Speybroeck,[†] Guy B. Marin,[‡] and Michel Waroquier*,[†]

Center for Molecular Modeling, Laboratory of Theoretical Physics, Ghent University, Proeftuinstraat 86, B-9000 Gent, Belgium, and Laboratorium voor Petrochemische Techniek, Ghent University, Krijgslaan 281-S5, B-9000 Gent, Belgium

Received: January 4, 2005; In Final Form: February 4, 2005

Density functional theory (DFT) cluster calculations were used to describe bifunctional acid−base properties of amine-substituted zeolites containing a Brønsted acid site. Preliminary results (*J. Am. Chem. Soc.* **2004**, *126*, 9162) indicated that efficient use of both functional groups might lead to a substantial lowering of activation barriers. In this paper, comparison is made between the alkoxide formation in zeolites containing only oxygen bridges and alkylammonium formation on the bridging NH groups in amine-functionalized zeolites for various guest species, such as methanol, ethene, and chloromethane. The amine functionalization only lowers barriers for SN_2 type reactions with otherwise highly strained transition states, as is the case for chloromethane. In these new materials more basic sites are introduced into the zeolite framework, enabling optimal linear SN_2 type transition states incorporating various T sites.

1. Introduction

Zeolites are microporous crystalline aluminosilicates, built from corner-sharing SiO_4 and AlO_4 tetrahedra interlinked through common oxygen atoms, giving rise to complex three-dimensional networks of channels, cages, and rings. These solid-state catalysts portray a wide variety of properties and applications (ranging from petroleum cracking to fine chemical synthesis), due mainly to their shape-selectivity and Brønsted acid sites that have the form ≡Si−OH−Al≡.[1]

Recent research has focused on extending the range of their applications by a well-chosen organic functionalization, altering the surface properties that control interaction with various guest species.[2] Manipulating these properties by replacing small parts of the zeolite structure by selected organic groups could create new catalytically active sites, allowing these novel materials to promote a broad range of reactions with potentially improved selectivity. Efforts in incorporating organic sites into the structure of microporous zeolites have not been straightforward. While first attempts using organosilanes with pendant organic groups succeeded in attaching, e.g., phenethyl groups into zeolite structures covalently bonded to framework silicon atoms,[3,4] the process was limited to certain zeolite structures. More importantly, even though a significant advance in widening the range of possible applications was made, the rather large organic groups tended to stick out of the framework, consequently blocking the molecular-sized pores. Increasing the density of organic groups in these organic-functionalized molecular sieves (OFMSs) led to two competing effects: not only a beneficial increase in amount of active centers but also a detrimental increase in diffusional limitations.

The problem of micropore clogging was eliminated when Yamamoto et al. succeeded in synthesizing LTA and MFI frameworks incorporating organic groups directly into the zeolite structure by partially superseding a lattice oxygen atom by a methylene group.[5] These organic−inorganic hybrid zeolites containing organic groups as lattice, or ZOLs, were synthesized from bis(triethoxysilyl)methane (BTESM). While the organic CH_2 groups significantly altered the adsorption properties of the zeolite, the methylene groups were not catalytically active, and chemically interesting materials are probably at least a generation off. Furthermore, the CH_2-substituted zeolites contained intrapore ≡Si−CH_3 moieties in addition to the bridging ≡Si−CH_2−Si≡ groups. This raised the question of whether these end groups were necessary to relieve induced strain due to the substitution or whether they were merely impurities, subject to synthesis conditions. Inspired by these results, Astala and Auerbach provided evidence through periodic DFT calculations that zeolites can accommodate not only methylene, but also amine groups at high concentrations with minimal strain.[6] They concluded that neighboring oxygen bridges easily absorbed the strain induced by the isoelectronic substitution. As opposed to methylene-functionalized zeolites, these amine-functionalized zeolites might possess chemically interesting properties. Theoretically determined adsorption energies of typical guest molecules such as NH_3 and BF_3 indicate that ≡Si−NH−Si≡ groups are significantly stronger Lewis bases than the usual ≡Si−O−Si≡ bridges, while ≡Al−NH_2−Si≡ groups show weaker Brønsted acid properties compared to ≡Al−OH−Si≡.[6] Though recently several research groups have succeeded in post-synthesizing nitrogen-containing mesoporous and microporous materials,[7−10] the crystallographic structure and true nature of the basic behavior of these novel materials is still under debate. Conclusive evidence of pure ZOL materials containing NH bridges directly incorporated into the zeolite framework remains to be reported.

The Lewis base properties of amine-modified zeolites are catalytically interesting in their own right; even more intriguing is the combination with well-known Brønsted acid sites due to aluminum impurities, which might lead to a dramatic increase in bifunctional acid−base properties. The zeolite framework would act as a unique host, providing both strong acid and base groups near a single active site. The prospective of improving

* To whom all correspondence should be addressed. Fax: 32 (0) 9 264 65 60. Email: michel.waroquier@UGent.be.
[†] Center for Molecular Modeling.
[‡] Laboratorium voor PetrochemischeTechniek.

10.1021/jp050032e CCC: $30.25
Published on Web 03/25/2005

both functional sites simultaneously demonstrates the necessity of a detailed theoretical study of the chemical behavior of neighboring Brønsted acid and Lewis base sites, providing useful guidelines for actual synthesis of these novel materials. First results of the interaction of chloromethane with small 4T and 5T clusters, as published in a previous communication,[11] show that amine modification of zeolites is capable of drastically lowering energy barriers for reactions in which both a Brønsted acid and a Lewis base site play a decisive role (e.g., for the formation of an intermediate alkoxide species). In the same paper, a study of proton mobility in these small clusters reveals that both strong acid and base sites will be present, providing the amine moiety is not located on the aluminum site. The combination of fully oxygen-surrounded aluminum sites and nearby ≡Si−NH−Si≡ bridges opens up the possibility of acid−base catalyzed reactions that are not solely centralized around the aluminum defect, but in which two T sites are involved. In this follow-up paper we will extend the brief results of our previous communication and discuss the interaction of amine-modified zeolites with several typical guest molecules such as methanol, chloromethane, and ethene. The zeolite environment is also modeled by larger 16T clusters and results will be discussed in more detail, providing conclusive information on possible use of these materials.

2. Alkoxide Formation in Zeolites

Many important zeolite-catalyzed reactions in the petrochemical industry make use of the acidic properties of protonated zeolites; most of these involve proton-transfer reactions as elementary steps (e.g., protonation of olefins and alcohols). Without any direct evidence, carbenium and carbonium ions were for a long time accepted as intermediate species stabilized in the polar zeolite surroundings by long-range electrostatic interactions (analogous to equivalent gas-phase reactions). Solid-state NMR and IR experiments indicate that adsorbed protonated hydrocarbons are not stable,[12,13] with exception of some cyclic cations with a delocalized positive charge and sterically inaccessible to framework oxygens.[14,15] Instead, protonation of adsorbed olefins and alcohols results in the formation of long-lived intermediate alkoxide species covalently bonded to the catalyst surface. Further arguments for the existence of such an alkoxide species inside zeolites can be found in ^{13}C MAS NMR studies.[16,17] Theoretical calculations using both the cluster approach and fully periodical techniques indicate that alkoxy species are local minima and thus stable intermediates, while carbenium ions act as transition states.[18−21] Actually, we must note that the true nature of reactive intermediates in reactions catalyzed by acid zeolites is still a matter of debate, certainly when large hydrocarbons are involved.[22] It can, however, be shown that for important industrial reactions, such as hydrocracking or catalytic cracking of these large hydrocarbons, the corresponding kinetic equations do not depend on the assumed nature of the reaction intermediates, i.e., alkoxides or carbenium ions.[23]

Methanol-to-gasoline (MTG) and methanol-to-olefin (MTO) processes are well-known in the production of higher hydrocarbons and other value-added products[24,25] and involve activation of the alcohol on the zeolite surface.[26−28] The methoxy intermediate is generated by dissociation of methanol over the acid site, resulting in a water molecule and a methyl group bound to a lattice oxygen atom. In light of sustainable energy production, early patents also report the possibility of converting halomethanes,[29] circumventing the costly formation of synthesis gas and reducing the number of byproducts. While the dissociative reaction mechanism involving an intermediate methoxy group is believed to be similar to the dissociation of methanol, subtle differences in the location of the acid proton in the transition state structure will have their consequences regarding catalytic properties of amine-modified zeolites, as will be demonstrated further on. Surface methoxy species formed from methanol or halomethanes also play an important role in the methylation of aromatics. On the other hand, ethylation of benzene can occur through a similar stepwise mechanism, starting with the protonation of adsorbed ethene by an acidic zeolite proton, generating a reactive ethoxide species.[30,31] The catalytic protonation of ethene and other olefins is often used to characterize the formation and reactivity of alkoxide species.

The unprotonated oxygen sites in the first coordination sphere of a framework tetrahedral aluminum show stronger Lewis base properties compared to ≡Si−O−Si≡ bridges, rendering the former the most likely sites for alkoxide species to be formed upon. It is believed that chemisorption proceeds in a concerted manner, controlled by a bifunctional (acid−base) mechanism, in which both the Brønsted acid site and the Lewis base properties of an oxygen-atom neighboring the acid site must be carefully balanced.[32] This stresses the importance of the basic centers on the acid−base pairs, since they play an active role in the stabilization of the charged intermediate species which should be formed in a wide range of reactions catalyzed by proton-exchanged zeolites. While earlier research focused mainly on improving the zeolite's acid properties, the basicity of the Lewis base site could be drastically enhanced by appropriate isoelectronic substitution. Amine substitution in particular might promote alkylammonium formation instead of alkoxide formation, subsequently influencing corresponding reaction barriers. In this paper, we report a theoretical study on the formation of an alkylammonium species starting from methanol, chloromethane, and ethene, and we will provide strong evidence that certain reaction barriers of important catalytic processes can be significantly lowered by appropriate substitution.

3. Method

3.1. Computational Details. Full geometry optimizations and frequency calculations for minimum energy and transition-state structures were performed within the Gaussian03 software package[33] using density functional theory (DFT). Zygmunt et al.[34] assessed the applicability of various readily available functionals for studying molecular adsorption in zeolite clusters and found that Becke's three-parameter B3LYP exchange-correlation functional[35] gives intermolecular energies and vibrational frequencies similar to those obtained using MP2. Their final conclusion stated that the B3LYP functional was the best choice for DFT treatment of zeolite clusters. Double ζ level basis sets at the 6-31g(d) level were used, and zero point energy corrections were included for all calculated energies. Activated complexes were validated to be true transition states and to exhibit only one imaginary frequency, whose normal mode corresponds with the reaction coordinate, while reactants and products were verified to contain no imaginary frequencies. For calculations using constraints, unavoidable additional imaginary frequencies (all with a magnitude smaller than 100 cm^{-1}) were checked to correspond with the motion of constrained atoms.

3.2. Cluster selection. The catalytic behavior of these novel materials is explored from a microscopic point of view, simulating the zeolite catalyst using the molecular cluster approach. We will refer to clusters as *n*T clusters, depending

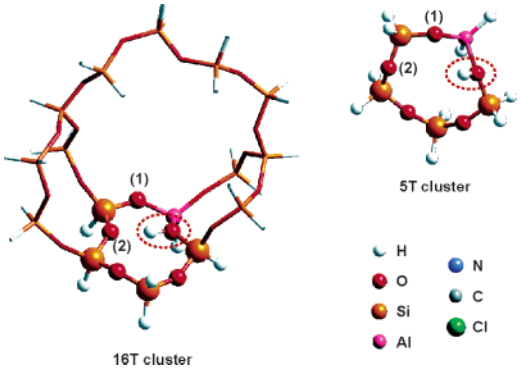

Figure 1. Full oxygen 5T cluster (21 atoms) and 16T cluster (62 atoms) with a single Brønsted acid site, used for ab initio calculations. (1) Oxygen site on aluminum tetrahedron. (2) Oxygen site opposite hydroxyl group. Red dotted line encircles acidic hydroxyl group. Color coding for different atoms is shown as well, including atoms occurring in following figures.

on the number *n* of tetrahedral Si or Al atoms incorporated in the cluster. The calculations were performed on a single ring of five tetrahedral atoms (5T cluster) and a larger 16T extension of this same ring to test the influence of a larger environment on the results. Both cluster types contain a Brønsted acid site, as shown in Figure 1. Even though these models do not fully represent the zeolitic environment, small clusters have shown to provide an adequate qualitative picture of chemical rearrangements that occur locally on the active site.[36−38] Cluster size has a distinct effect on quantitative properties, such as proton affinity and OH stretching frequencies,[39] but for a qualitative description of acid zeolite catalyzed reactions, 5T clusters or even smaller 4T clusters have proven to be sufficient. For example, Rozanska et al.[40] studied the isomerization and transalkylation of toluene and xylenes and found that the relative order of the activation energies is conserved when comparing results obtained using small 4T clusters and fully periodic calculations.

On the other hand, small clusters may correctly model the active site, but they do not fully incorporate structurally distinguishable properties of particular zeolites, and larger clusters are needed to capture pertinent features of specific zeolite structures. More representative 16T clusters, containing the initial 5T ring surrounded by a larger part of the zeolite framework, were used for more advanced calculations in order to check the validity of the 5T results. For the calculations on the 5T cluster no geometric constraints were imposed to verify the true nature of stationary points, i.e., absolute minima or saddle points. At this level of approximation we obtain molecular-type systems with atoms having a larger degree of freedom compared to the real active sites that are embedded in a solid framework. As a result, artificial deformations of the model occur in the smaller 5T cluster. The larger 16T cluster does not suffer from these shortcomings since the fixed volume approach (by constraining the 11 exterior Si atoms to crystallographic positions) was employed to preserve geometric integrity of the zeolite, thereby reducing the artificial deformation of the incorporated 5T ring. Dangling bonds, which in the authentic zeolite would connect the cluster with the rest of the solid, were saturated with hydrogen atoms in order to preserve electrostatic neutrality and spin multiplicity.

In reality, the entire zeolite framework stabilizes charged species, while neutral species are less affected. The calculated activation energies can be expected to decrease by a further 10−50% when the zeolite lattice is properly taken into account.[40−43] For the course of this paper, in which we are interested in a qualitative description of a material for which no experimental data are available, the two suggested clusters provide a reasonable compromise between realistic and computationally feasible models. The current investigation concentrates on protonated and amine-substituted ZSM-5, since this structure type can be synthesized over a wide range of Si/Al ratios. Moreover, Yamamoto et al.[5] already succeeded in synthesizing methylene-substituted MFI frameworks. The ZSM-5 (MFI) framework consists of two-dimensional intercrossing straight 10-ring channels in the [010] direction and sinusoidal channels in the [100] direction,[44] exhibiting crucial shape selective characteristics. The suggested cluster models do not incorporate the steric constraints needed for shape selectivity, but this is of minor importance as we only study the interaction with relatively small molecules.

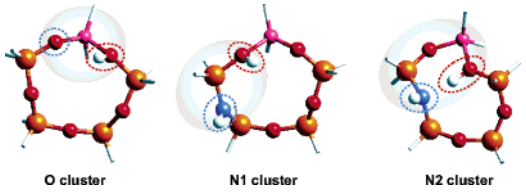

Figure 2. 5T clusters with terminating hydrogens displayed as cylinders. Red dotted line shows acid site, blue dotted line denotes basic site, while reactive area is visualized by gray background.

Following our previous communication,[11] we will compare three different acid−base combinations, as shown in Figure 2. As a reference to zeolites containing only oxygen bridges, we studied the O cluster with both the acid hydroxyl group and the basic oxygen atom located on the aluminum tetrahedron. Reactions based on bifunctional acid−base properties will be centralized around this single T-site. Direct comparison can be made with the N1 cluster, where the nitrogen substitution is one tetrahedral site removed from the aluminum defect, but the hydroxyl group and amine group are still located on the same T-site, albeit a silicon tetrahedron. The N2 cluster has a hydroxyl group located in the same position as the O cluster. Similar to the N1 cluster, the amine moiety is one oxygen bridge removed from the aluminum substitution. The main difference between N2 and O/N1 lies in the fact that the acid proton is now located opposite the hydroxyl group. Consequently, reactions incorporating both functional groups will span two separate T-sites instead of one, which has a major influence on transition state geometries.

4. Results and Discussion

4.1. Proton mobility. The fact that protonated zeolites such as H−Y and H−ZSM-5 exhibit strong acidic properties, suggests that protons may be able to jump among oxygens in an AlO_4 tetrahedron. This is confirmed by experimental studies suggesting that acidic protons are not fixed to a specific framework oxygen atom, but are quite mobile at elevated temperatures: NMR measurements on acidic zeolites reveal significant proton mobility with surprisingly low activation energies, depending on the zeolite and Si/Al ratio studied. For example, through variable temperature ^{1}H magic-angle spinning NMR studies of H−ZSM-5, Sarv et al. report an activation energy of 45 kJ/mol,[45] while Baba et al. report 17−20 kJ/mol.[46] For hydrated zeolites, proton mobility is known to be greatly enhanced by trace amounts of water in the micropores,[47] acting as proton vehicle molecules.

Two different types of proton motion must be distinguished: local on-site jumps between four atoms in the first coordination sphere of an aluminum atom and translational intersite motion

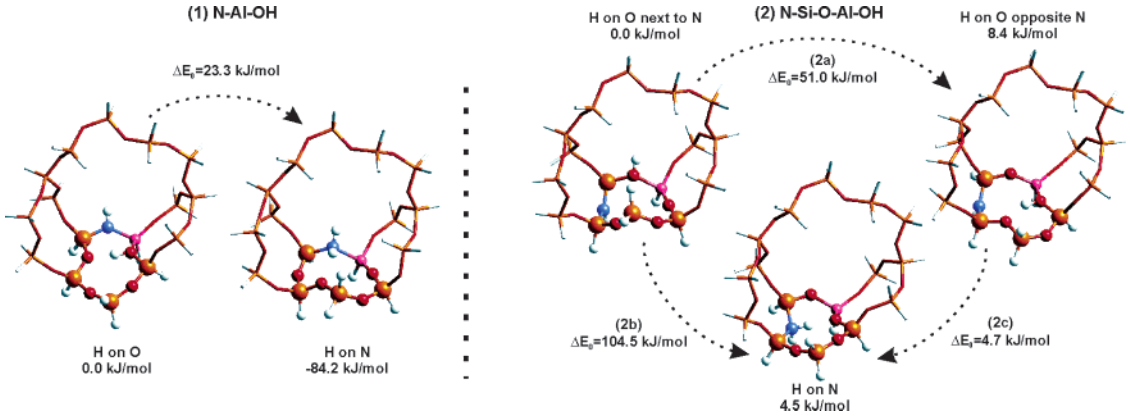

Figure 3. Geometry and energy (in kJ/mol) relative to a chosen reference state for different proton locations in amine-substituted 16T clusters. The (1) cluster has the nitrogen substitution located on the aluminum tetrahedron, while for the (2) cluster the amine moiety is located opposite the hydroxyl group.

between two different aluminum sites. In traditional zeolites, the on-site jumps are much more probable than translational jumps,[48] as in the latter case the protons would have to leave the AlO_4^- site and move to less basic bridging ≡Si−O−Si≡ sites. The presence of NH bridges in organic functionalized materials significantly alters these proton mobility properties. Additionally, the proton location is essential in exploring efficient relative positions for the NH bridge and Al site. Two distinct configurations are considered (Figure 3): a first cluster (1) with both OH and NH groups located at the same T atom, and a second cluster (2) with the nitrogen substitution occurring at a neighboring tetrahedral site. As indicated in Figure 3, all energies are relative to a chosen reference state.

Even though a much larger part of the zeolite was incorporated for the 16T cluster, qualitative results are identical to the 5T cluster.[11] For the cluster (1), in which the NH and OH functional groups are located in the first coordination sphere of the aluminum atom, amine protonation has a low activation energy of 23.3 kJ/mol and results in a thermodynamically favored configuration (−84.2 kJ/mol). This latter configuration, containing a mildly acidic NH_2 group exhibits nonoptimal acid−base properties.

To obtain combined optimal acid and base properties for a thermodynamically favored zeolite, it is essential to separate the amine moiety from the aluminum site, e.g., to have the configuration (2) as shown in Figure 3. The on-site proton hopping barrier between two basic oxygens (2a) is hardly influenced by the amine substitution, with an energy barrier of 51 kJ/mol.[49] Proton jumps between OH and NH substituted sites located in the first coordination sphere of a silicon atom (path 2b) are highly activated by 104.5 kJ/mol, comparable to equivalent intersite proton jumps in full oxygen zeolites.[48] A much more efficient channel leading to a NH_2 substitution is characterized by an almost barrierless proton jump of 4.7 kJ/mol crossing the 5T ring (2c). This last jump to a "free" proton, in the sense that it is no longer located on the aluminum T-site, is easily made because the proton bound to the oxygen atom forms a hydrogen bond with the opposite nitrogen atom and vice versa. Whereas in traditional zeolites jumps to non-aluminum oxygen bridges are less probable,[48] this is not the case for amine-substituted zeolites. All three possible configurations as shown in (2) have comparable binding energies and will be equally likely to occur. As opposed to the ≡Al−NH−Si≡ cluster (1) in Figure 3, there is a reasonable probability of the nitrogen site not being protonated. It is exactly this coexistence of the hydroxyl group with the amine group that allows for a drastic improvement in bifunctional acid−base properties.

SCHEME 1

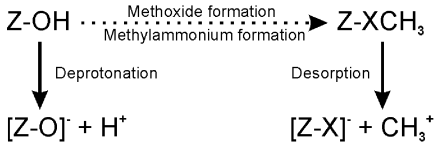

TABLE 1: Heats of Deprotonation and CH_3^+ Desorption for 5T and 16T Clusters (cluster terminology defined in Figure 2)

B3LYP/6-31g(d) (kJ/mol)	deprotonation		CH_3^+ desorption	
	5T	16T	5T	16T
O	1259.8	1231.0	791.7	763.4
O2			689.7	667.4
N1	1265.4	1226.2	775.7	762.1
N2	1263.3	1234.6	775.7	765.7

4.2. Characterization of Acidic and Basic Properties. All reactions studied in this paper proceed through a bifunctional (acid−base) mechanism and a careful balancing of acid and base properties is crucial. In this section, we will quantify these specific aspects of the various sites for our different cluster models. The acid properties can be quantified by calculating the enthalpy of deprotonation or by calculating the adsorption heat of ammonia.[39,50,51] In this paper, we will use the former scale of acidity, as illustrated in Scheme 1. Since the calculations are performed on a finite model of the active site, the results will contribute substantially to our knowledge of Brønsted acidity of organic functionalized materials but will not differentiate between the acidities of Brønsted acid sites in different crystallographic environments.[42] It is solely our intention to obtain insight into the factors contributing to acidity caused by changes in the local environment, i.e., the difference between traditional zeolites with only oxygen bridges and new materials with amine substitutions.

The results for deprotonation energies defined as $E_{DP} = E_0([Z-O]^-) + E_0(H^+) - E_0(Z-OH)$ are summarized in Table 1. The absolute values obtained in the larger 16T cluster are approximately 20−30 kJ/mol lower than for the smaller 5T cluster, illustrating the stabilizing effect of the larger environment on the positive charge. No clear distinction can be made between the acidity of oxygen sites in traditional zeolites or NH-substituted clusters. Only variations of the order of 5 kJ/

mol can be noted, and finite cluster calculations are not accurate enough to distinguish between such small energy differences.

To characterize the Lewis base properties of these materials, i.e., the ability of donating an electron pair, we calculate the sorption energies of CH_3^+ according to Scheme 1. Note that the starting configuration is negatively charged due to the presence of an unsaturated aluminum substitution. The definition of basicity we use is slightly different from the basicity scale employed by Astala and Auerbach,[6] who used the sorption energy of BF_3 on ≡Si−X−Si≡ as a measure of basicity for a neutral starting configuration without aluminum defect. As the studied reactions all involve the formation of an alkoxide species, the present definition is more appropriate for our cause and results are given in Table 1. A stronger binding of the methyl group to the basic group might have a significant lowering effect on reaction barriers. On the other hand, the formation of an intermediate methoxide species is usually the first step in the multiple-step reaction process. If the methyl group is too strongly bound it might not be reactive enough for these following steps to occur.

It was shown above that NH substitutions bonded to the aluminum atom (site (1) in Figure 3) are thermodynamically prone to protonation, resulting in nonoptimal acid−base properties. Thus, for the amine-modified zeolites, methylammonium formation was always considered at site (2). For traditional zeolites with only oxygen bridges, it is commonly accepted that a methoxide species is formed on the more basic oxygen site (1) as shown in Figure 1, located next to the aluminum atom. However, for proper comparison with the results on the amine-substituted clusters, we also calculated desorption energies for a methoxide species formed at site (2), from now on referred to as the O2 cluster. As shown in Table 1, the desorption energy $E_{DS} = E_0([Z-X]^-) + E_0([CH_3]^+) - E_0([Z-XCH_3])$ (where X equals O or NH depending on the zeolite functionalization) for the O2 cluster is substantially lower than for a methoxide species formed on the aluminum tetrahedron. The energy difference of about 100 kJ/mol indicates the cost of charge separation due to the positive methoxy group not being located near the negatively charged aluminum defect. Sorption energies for the NH-substituted clusters with the methylammonium species also formed at site (2) are about 100 kJ/mol higher compared to the O2 cluster, due to the strong basic character of the amine bridge. The sorption energy for CH_3^+ at the oxygen atom located on site (1) is of the same order of magnitude as the corresponding values for nitrogen-bridged zeolites. Apparently, two effects largely contribute to the sorption energy: (i) the basicity of the nitrogen or oxygen bridge and (ii) the energy cost needed for charge separation between the CH_3^+ group and the AlO_4^- tetrahedron. For the amine-modified zeolites, these effects seem to simply cancel each other out. Also note that due to the charge separation effects, the methylammonium group is just as readily available for succeeding reaction steps as the methoxide species is.

In conclusion, we find all clusters to be of similar Brønsted acidity, while the formed C−O bond for the oxygen site (1) is of equal strength as the C−N bonds formed upon site (2). More importantly, based on these results, any lowering of reaction barriers for nitrogen-substituted zeolites cannot solely be ascribed to the strong Lewis basic properties of the nitrogen group.

4.3. Interaction with Chloromethane. We studied the first step of the dissociative mechanism in the conversion of chloromethane to hydrocarbons over acidic zeolite catalysts such as H−ZSM-5. Using traditional zeolites, containing only oxygen bridges, this first step follows a concerted reaction mechanism.[52] Initially the halomethane is adsorbed to the cluster. Next, in a single combined step, the halomethane dissociates as the methyl group is transferred to a zeolite oxygen atom through a carbenium-ion like transition state, leading to the formation of a surface methoxide species and hydrochloric acid. Afterward, this framework-bonded methoxide is available for transfer to a hydrocarbon. No stable charged intermediates were found during the reaction. Introducing NH bridges into the silicon/aluminum framework does not severely alter the reaction mechanism, except for the formation of a methylammonium species instead of a methoxide species. The reactions were studied on the three clusters shown in Figure 2: the traditional formation of a methoxide species in an exclusively oxygen-bridged zeolite, with the transition state localized around one tetrahedral site (Al), the formation of a methylammonium group, also centered around a single T-site (Si), and the formation of a methylammonium group spanning two neighboring tetrahedral sites (Al+Si). Stationary points are shown in Figure 4 and energetic results of the adsorbed species and activated complexes are summarized in Table 2. Energies are always referred to the ground-state energy of the adsorbed reactants.

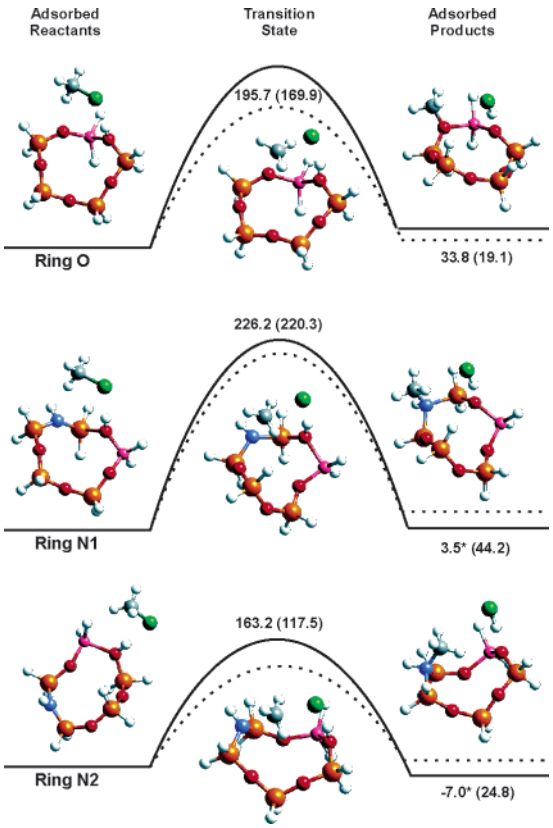

Figure 4. Stationary points for methoxide or methylammonium formation from chloromethane for various initial configurations. Energies are given in kJ/mol and are relative to the energy of the adsorbed reactants. 16T cluster results are shown with a solid line, while the dotted line represents the 5T cluster results (value between brackets). 16T energies marked with an asterisk are the result of a hydrogen bond with a framework oxygen atom not present in the 5T cluster.

As expected, while they substantially differ quantitatively speaking, the 5T and 16T clusters reveal similar qualitative information. The main difference among the three clusters can be seen in the energy barrier, large enough to conclude following order: $\Delta E_0(N2) < \Delta E_0(O) < \Delta E_0(N1)$. Compared to the traditional methoxide formation (cluster O; 5T: 169.9 kJ/mol; 16T: 195.7 kJ/mol), the nitrogen substitution yields a substantial improvement in catalytic properties, but only for the reaction

TABLE 2: Calculated DFT Energies + ZPE for Stationary Points in Reference to Corresponding Energy of Adsorbed Reactants[a]

B3LYP/6-31g(d) (kJ/mol)		CH_3Cl		CH_3OH		C_2H_4	
		5T	16T	5T	16T	5T	16T
O	R	16.6	13.7	68.3	57.4	13.4	17.0
	AR	0.0	0.0	0.0	0.0	0.0	0.0
	TS	169.9	195.7	199.8	*146.7	96.6	96.4
	AP	19.1	33.8	37.0	38.6	−52.7	−49.0
	P	45.2	41.9	80.5	69.1		
N1	R	29.2	11.8	54.3	68.9	11.9	18.4
	AR	0.0	0.0	0.0	0.0	0.0	0.0
	TS	220.3	226.2	165.8	*147.4	141.0	125.3
	AP	44.2	*3.5	42.3	*40.9	−11.7	−26.4
	P	62.6	36.4	88.1	77.1		
N2	R	11.0	9.8	40.9	81.0	6.5	22.5
	AR	0.0	0.0	0.0	0.0	0.0	0.0
	TS	117.5	163.2	150.3	181.4	124.3	125.7
	AP	24.8	*−7.0	26.8	*35.9	−19.2	−49.6
	P	59.1	23.2	72.6	78.1		

[a] 16T energies marked with an asterisk are the result of a hydrogen bond between the adsorbed species and a framework oxygen atom not present in the 5T cluster.

TABLE 3: Geometric Parameters of CH_3Cl Transition States Compared to Ideal SN_2 Values (basic site denoted by X: X=O or NH)

transition state	O		N1		N2		ideal
CH_3Cl (°)	5T	16T	5T	16T	5T	16T	SN_2
$C-H_a-H_b-H_c$ dihedral	7.5	10.3	9.1	11.5	5.4	7.9	0.0
Cl−C−X angle	145.0	144.7	140.3	144.2	172.6	168.0	180.0
$Cl-C-H_a$ angle	109.1	108.0	112.6	108.0	91.1	93.0	90.0
$Cl-C-H_b$ angle	75.9	72.2	75.4	72.7	84.9	82.3	90.0
$Cl-C-H_c$ angle	76.2	76.8	71.7	74.6	86.0	83.0	90.0
$X-C-H_a$ angle	105.9	107.2	107.0	107.7	95.8	98.5	90.0
$X-C-H_b$ angle	88.4	89.8	89.1	89.5	90.0	89.1	90.0
$X-C-H_c$ angle	88.3	90.1	89.1	91.7	92.7	94.5	90.0

mechanism spanning two T-sites (cluster N2; 5T: 117.5 kJ/mol; 16T: 163.2 kJ/mol). As the process is concerted and the acidity of the OH group is not significantly altered (Table 1), one would at first sight ascribe the decrease in activation energy to the stronger basic character of the NH group. If basicity of the nitrogen group were the only determining factor, the N1 cluster would also show a lowering in activation energy. On the contrary, the opposite is observed (cluster N1; 5T: 220.3 kJ/mol; 16T: 226.2 kJ/mol). As demonstrated earlier, two effects contribute to the stability of the methoxide or methylammonium group: basicity of the basic X site (X = O or NH) and the energy needed for charge separation. These effects cancel each other out for the N2 cluster and lead to an equally stable N-C bond for the N1 site. To explain the decrease in activation energy, we must look at geometrical features instead.

As can be seen in Figure 4, the crucial difference between cluster N2 and clusters N1 and O lies in the geometry of the transition state: spanning two tetrahedral sites is energetically favorable to constraining the reaction to a single T-site. For optimal interaction, the methyl group should be in a planar conformation perpendicular to the axis connecting Cl, C and the basic site X (X=O or NH), transferring the methyl-group like a typical SN_2 reaction through an umbrella-like inversion. For the fully oxygen-surrounded clusters, the transition state structure is largely distorted in order to interact with both catalyst donor atoms. However, an effective SN_2 intermediate requires a full overlap among the orbitals of the nucleophiles and the active 2p orbital of the carbon atom in the planar methyl group. For O and N1, this requirement is not fulfilled, as shown in Table 3, and the transition state structure is rather unstable. For the N2 cluster, the situation is completely different: the methyl group is indeed in a planar configuration as in typical SN_2 reactions, but more importantly the Cl, C, and N atoms are almost collinear. This proves that the strong basicity of the nitrogen atom does not directly lower the reaction barrier, but merely provides a more accessible basic site for a typical SN_2 reaction to occur. Apparently, the profit of a linear transition state outweighs the cost of charge separation. The N1 cluster on the other hand suffers from both disadvantages: a strained transition state combined with charge separation, resulting in the highest energy barrier for this reaction.

TABLE 4: Geometric Parameters of CH_3OH Transition States Compared to Ideal SN_2 Values (basic site denoted by X: X=O or NH)

transition state	O		N1		N2		ideal
CH_3OH (°)	5T	16T	5T	16T	5T	16T	SN_2
$C-H_a-H_b-H_c$ dihedral	−12.1	−4.0	−3.0	−2.8	−3.0	−3.4	0.0
O−C−X angle	175.2	167.8	172.0	171.4	172.0	164.6	180.0
$O-C-H_a$ angle	97.2	96.0	95.5	95.2	95.5	96.6	90.0
$O-C-H_b$ angle	94.5	88.5	90.6	88.0	90.6	93.2	90.0
$O-C-H_c$ angle	96.8	91.7	88.3	91.0	88.3	85.4	90.0
$X-C-H_a$ angle	86.1	96.2	92.4	93.4	92.4	96.5	90.0
$X-C-H_b$ angle	86.9	84.7	84.6	87.2	84.6	81.1	90.0
$X-C-H_c$ angle	78.6	83.3	88.6	85.2	88.6	87.5	90.0

4.4. Interaction with Methanol. A similar concerted reaction path can be calculated for zeolite acid−base interaction with methanol.[53,54] Initially the methanol molecule is adsorbed to the cluster, after which it dissociates as the methyl group is transferred to a zeolite oxygen atom through a carbenium-ion-like transition state, leading to the formation of a surface methoxide species and a water molecule. The corresponding transition state is a methoxonium-like ion-pair complex. However, compared to chloromethane, the equivalent reaction with methanol shows several distinct differences, as not all bonds are broken or formed to the same extent in the transition structure. The bond between the acid proton and the hydroxyl group is already formed, while bond breaking of the methyl group and the hydroxyl group and bond making between methyl group and zeolite are simultaneously in process. This specific detail is crucial for the geometric features of the transition state. As opposed to chloromethane, the original acid zeolite proton is no longer confined to the zeolite oxygen atom and has the ability to reorient itself in order to form a geometrically favored linear SN_2-like transition structure (Table 4). The methyl umbrella is already slightly inverted, visible through a negative $C-H_a-H_b-H_c$ dihedral. This asynchronous pathway does not result in the formation of stable charged intermediates. Reaction schemes are shown in Figure 5 and the energies for all stationary points are given in Table 2. This linear transition state differs from previously reported small cluster calculations[53,54] where only the aluminum tetrahedron was modeled. In these models, the only available basic groups were located next to the acidic hydroxyl group and only a highly strained transition state could be found. Zicovich-Wilson et al.[55] mentioned this limitation of small cluster models and reported an unstrained multicenter transition state, similar to the transition states we obtained, with a methoxide species formed on a less basic ≡Si−O−Si≡ bridge. Recently, Vos et al.[56] also reported an almost linear methoxonium-like SN_2 transition state for calculations on a 4T cluster, similar to the one we obtained.

From a geometrical point of view it makes no difference whether the reactions occur at one or two T sites (all active sites show nearly identical features), and thus similar reaction

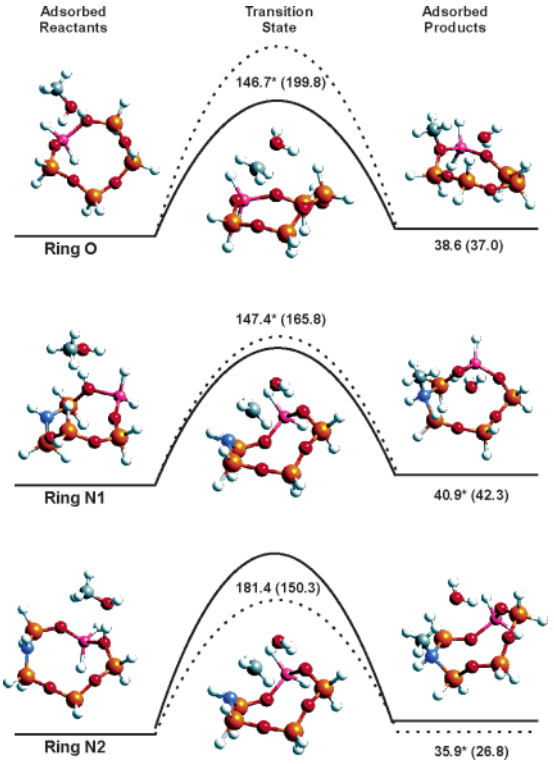

Figure 5. Stationary points for methoxide or methylammonium formation from methanol for various initial configurations. Energies (in kJ/mol) are relative to the energy of the adsorbed reactants. 16T cluster results are shown with a solid line, while the dotted line represents the 5T cluster results (value between brackets). 16T energies marked with an asterisk are the result of a hydrogen bond with a framework oxygen atom not present in the 5T cluster.

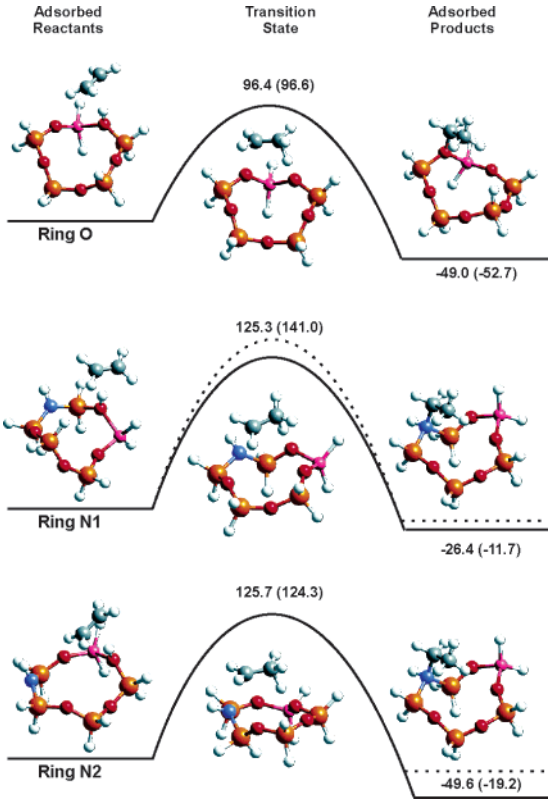

Figure 6. Stationary points for ethoxide or ethylammonium formation from ethene for various initial configurations. Energies (in kJ/mol) are relative to the energy of the adsorbed reactants. 16T cluster results are shown with a solid line, while the dotted line represents the 5T cluster results (value between brackets).

barriers are expected for O, N1, and N2 clusters. This is not the case due to the appearance of hydrogen bonds that stabilize the transition structures and adsorbed species. For the 5T cluster, the oxygen ring shows a highly energetic transition state (199.8 kJ/mol), whereas the N1 and N2 transition states are much lower in energy. For the N-substituted clusters, the water molecule always forms a hydrogen bond with the opposite basic oxygen atom at the aluminum T site. This is not the case for the oxygen bridged zeolite, and no hydrogen bonds were formed. By incorporating a larger part of the zeolite environment (16T), the water molecule in the O cluster also stabilizes in the transition state by formation of a hydrogen bond with one of the framework oxygen atoms that was nonexistent in the 5T cluster. The differences in activation energies between N1 and N2 clusters must be mainly ascribed to variations in adsorption energies of the reactants and slight deformations in ideal SN_2 parameters. One must, however, be extremely cautious with the energetics of clusters containing weak hydrogen bonds with framework oxygen atoms, as it is commonly known that accurate values of these energies require incorporation of large extents of the zeolite cluster. Furthermore, density functional theory is known for its severe limitations in correctly describing these weak interactions.

For the interaction with methanol, we can conclude that the system will automatically take on the optimal SN_2-type transition state, with the water molecule hydrogen bonded to a framework oxygen atom. Even though reaction barriers are not reduced, amine functionalization of the catalyst is far from pointless. The amine groups will provide more basic sites and will facilitate the formation of multicenter transition states in the zeolite micropores.

4.5. Interaction with Ethene. We will now discuss the zeolite-catalyzed protonation of a doubly bonded system such as ethene, which has been the subject of numerous theoretical studies.[57−62] The protonation of olefins such as ethene starts with the formation of a weak π-complex, after which the olefin double bond is attacked by the zeolite acid proton. Upon chemisorption, a covalent C(olefin)−O(zeolite) bond is formed, producing a stable alkoxide σ-complex. The chemisorption reaction is strongly exothermic. The reaction profiles, which are similar for various clusters, are shown in Figure 6, whereas energies for stationary points are given in Table 2.

The reaction mechanism differs from previously discussed examples such as chloromethane and methanol, as it does not occur through a SN_2 mechanism. For this reaction, charge separation dominates reaction kinetics, while the 1T transition state is hardly strained. As a result, the fully oxygen surrounded zeolite has the lowest activation barriers: for the amine substituted clusters there is still the effect of charge separation between the aluminum atom and the positively charged $[CH_3-CH_2]^+$ species, resulting in higher activation energies. As the main ingredient for activation barrier lowering, i.e., relief of steric hindrance in the transition state, does not occur, it is clear that the amine moiety will not improve the catalytic performance.

5. Conclusions

We performed a series of both 5T and 16T cluster calculations using density functional theory to describe the interaction between amine-modified zeolites and various guest species. We especially focused on combining a strong Lewis base amine site with a Brønsted acid proton near an aluminum substitution,

to explore whether this specific combination would substantially improve bifunctional acid−base properties of the catalyst. As the formation of an intermediate alkoxy species is a typical reaction step in the conversion of small alcohols and olefins on protonated zeolites, we compared the alkoxide formation in traditional zeolites (containing only oxygen bridges) to alkylammonium formation on the bridging NH groups in amine-functionalized zeolites. Furthermore, these specific reactions are characterized not only by the acidity of the hydroxyl group but also by the Lewis base properties of the neighboring site responsible for the crucial zeolite−carbon bond.

A study of proton mobility in these novel materials revealed that amine substitutions on the aluminum tetrahedron are easily protonated, resulting in a weakly acidic NH_2 group and a moderately basic oxygen atom. However, if the presence of nitrogen−aluminum bridges could be minimized during synthesis, a proton will only sporadically contaminate the nitrogen sites and the two strong functional groups are able to coexist. By calculating heats of deprotonation, we found that amine modification of the zeolite does not alter the acidic properties of the hydroxyl group. Surprisingly, we also found that the effect of charge separation between the positively charged alkylammonium species and the $[AlO_4]^-$ tetrahedron and the effect of a stronger basic nitrogen atom compared to an oxygen atom simply cancel each other out. This means that the N−C bond in amine-modified zeolites is no stronger than the O−C bond in fully oxygen-bridged zeolites. Consequently, due to the fact that the amine moiety cannot be located on the aluminum tetrahedron to prevent protonation, the amine site does not necessarily promote alkylammonium formation. Because of the delicate balance between these two effects, geometric features of the transition state will determine whether amine functionalization enhances catalytic performance or not.

In the case of chloromethane, our microscopic calculations present strong evidence that amine-modified zeolites are capable of drastically lowering energy barriers. However, this lowering of activation barriers is restricted to reactions where transition states centered on the aluminum defect are highly strained. For these SN_2 type reactions, the possibility of a multicenter transition state spanning two adjacent T-sites allows for an energetically preferable configuration. Methanol, on the other hand, will always try to take on the optimal linear SN_2 transition state. Therefore, supplying additional amine sites will not lower the reaction barriers as in the case of chloromethane. Nevertheless, amine functionalization will still lead to a significant progress in catalytic performance, as this unique way of providing more basic sites will also improve the chances of an adsorbed molecule undergoing successful reaction, allowing more efficient use of the zeolite acid site and the surrounding environment. However, it remains uncertain whether the gain in catalytic properties would outweigh the expensive cost of actual synthesis. Finally, we found that for reactions such as the protonation of ethene, which do not exhibit any strain in the 1T transition state structure, amine-modified zeolites are only capable of providing more basic sites. Without the gain of a more preferable transition state geometry, activation barriers for reaction mechanisms that are not centered around the aluminum atom will be slightly higher.

In conclusion, we state that it is certainly worth synthesizing Al-containing amine-modified zeolites in the light of novel catalytic materials, and we believe that organic functionalization of zeolites will mean a huge advance in future tailoring of catalysts for specific reactions.

Acknowledgment. This work is supported by the Fund for Scientific Research − Flanders (FWO) and the Research Board of Ghent University.

Supporting Information Available: Cartesian coordinates of all adsorbed species and transition states (5T). This material is available free of charge via the Internet at http://pubs.acs.org.

References and Notes

(1) Corma, A. *Chem. Rev.* **1995**, *95*, 559−614.
(2) Jones, C. W. *Science* **2003**, *300*, 439−440.
(3) Jones, C. W.; Tsuji, K.; Davis, M. E. *Nature* **1998**, *393*, 52−54.
(4) Jones, C. W.; Tsapatsis, M.; Okubo, T.; Davis, M. E. *Microporous Mesoporous Mater.* **2001**, *42*, 21−35.
(5) Yamamoto, K.; Sakata, Y.; Nohara, Y.; Takahashi, Y.; Tatsumi, T. *Science* **2003**, *300*, 470−472.
(6) Astala, R.; Auerbach, S. M. *J. Am. Chem. Soc.* **2004**, *126*, 1843−1848.
(7) Ernst, S.; Hartmann, M.; Sauerbeck, S.; Bongers, T. *Appl. Catal. A: General* **2000**, *200*, 117−123.
(8) Xia, Y.; Mokaya, R *Angew. Chem., Int. Ed.* **2003**, *42*, 2639−2644.
(9) Xiong, J.; Ding, Y.; Zhu, H.; Yan, L.; Liu, X.; Lin, L. *J. Phys. Chem. B* **2003**, *107*, 1366−1369.
(10) Zhang, C.; Xu, Z.; Wan, K.; Liu, Q. *Appl. Catal. A: General* **2004**, *258*, 55−61.
(11) Lesthaeghe, D.; Van Speybroeck, V.; Waroquier, M. *J. Am. Chem. Soc.* **2004**, *126*, 9162−9163.
(12) Aronson, M. T.; Gorte, R. J.; Farneth, W. E.; White, D. *J. Am. Chem. Soc.* **1989**, *111*, 840−846.
(13) Haw, J. F.; Richardson, B. R.; Oshiro, I. S.; Lazo, N. D.; Speed, J. A. *J. Am. Chem. Soc.* **1989**, *111*, 2052−2058.
(14) Haw, J. F. *Phys. Chem. Chem. Phys.* **2002**, *4*, 5431−5441.
(15) Bjørgen, M.; Bonino, F.; Kolboe, S.; Lillerud, K. P.; Zecchina, A.; Bordiga S. *J. Am. Chem. Soc.* **2003**, *125*, 15863−15868.
(16) Bosacek, V. *J. Phys. Chem.* **1993**, *97*, 10732−10737.
(17) Philippou, A.; Salehirad, F.; Luigi, D. P.; Anderson, M. W. *J. Chem. Soc., Faraday Trans.* **1998**, *94*, 2851−2856.
(18) Kazansky, V. B. *Catal. Today* **1999**, *51*, 419−434.
(19) Benco, L.; Hafner, J.; Hutschka, F.; Toulhoat, H. *J. Phys. Chem. B* **2003**, *107*, 9756−9762.
(20) Bhan, A.; Joshi, Y. V.; Delgass, W. N.; Thomson, K. T. *J. Phys. Chem. B* **2003**, *107*, 10476−10487.
(21) Boronat, M.; Viruela, P. M.; Corma, A. *J. Am. Chem. Soc.* **2004**, *126*, 3300−3309.
(22) Thybaut, J. W.; Narasimhan, C. S. L.; Marin, G. B.; Denayer, J. F. M.; Baron, G. V.; Jacobs, P. A.; Martens, J. A. *Catal. Lett.* **2004**, *94*, 81−88.
(23) Yaluris, G.; Madon, R.; Dumesic, J. *J. Catal.* **1999**, *186*, 134−146.
(24) Meisel, S. L.; McCullough, J. P.; Lechthaler, C. H.; Weisz, P. B. *Chemtech* **1976**, *6*, 86−89.
(25) Chang, C. D. *Hydrocarbons from methanol*; Marcel Dekker: New York, 1983.
(26) Wang, W.; Seiler, M.; Hunger, M. *J. Phys. Chem. B* **2001**, *105*, 12553−12558.
(27) Wang, W.; Buchholz, A.; Seiler, M.; Hunger, M. *J. Am. Chem. Soc.* **2003**, *125*, 15260−15267.
(28) Dewaele, O.; Geers, V. L.; Froment, G. F.; Marin, G. B. *Chem. Eng. Sci.* **1999**, *54*, 4385−4395.
(29) (a) Butter, A. A.; Jurewicz, A. T.; Kaeding, W. W. U.S. Patent 3,894,407, July 8, 1975. (b) Kaiser S. W. International Patent WO 86/045777, Aug. 14, 1986.
(30) Degnan, T. F., Jr.; Smith, C. M.; Venkat, C. R. *Appl. Catal. A: General* **2001**, *221*, 283−294.
(31) Namuangruk, S.; Pantu, P.; Limtrakul, J. *J. Catal.* **2004**, *225*, 523−530.
(32) van Santen, R. A.; Kramer, G. J. *Chem. Rev.* **1995**, *95*, 637−660.
(33) Frisch, M. J.; Trucks, G. W.; Schlegel, H. B.; Scuseria, G. E.; Robb, M. A.; Cheeseman, J. R.; Montgomery, J. A., Jr.; Vreven, T.; Kudin, K. N.; Burant, J. C.; Millam, J. M.; Iyengar, S. S.; Tomasi, J.; Barone, V.; Mennucci, B.; Cossi, M.; Scalmani, G.; Rega, N.; Petersson, G. A.; Nakatsuji, H.; Hada, M.; Ehara, M.; Toyota, K.; Fukuda, R.; Hasegawa, J.; Ishida, M.; Nakajima, T.; Honda, Y.; Kitao, O.; Nakai, H.; Klene, M.; Li, X.; Knox, J. E.; Hratchian, H. P.; Cross, J. B.; Adamo, C.; Jaramillo, J.; Gomperts, R.; Stratmann, R. E.; Yazyev, O.; Austin, A. J.; Cammi, R.; Pomelli, C.; Ochterski, J. W.; Ayala, P. Y.; Morokuma, K.; Voth, G. A.; Salvador, P.; Dannenberg, J. J.; Zakrzewski, V. G.; Dapprich, S.; Daniels, A. D.; Strain, M. C.; Farkas, O.; Malick, D. K.; Rabuck, A. D.; Raghavachari, K.; Foresman, J. B.; Ortiz, J. V.; Cui, Q.; Baboul, A. G.; Clifford, S.; Cioslowski, J.; Stefanov, B. B.; Liu, G.; Liashenko, A.; Piskorz,

P.; Komaromi, I.; Martin, R. L.; Fox, D. J.; Keith, T.; Al-Laham, M. A.; Peng, C. Y.; Nanayakkara, A.; Challacombe, M.; Gill, P. M. W.; Johnson, B.; Chen, W.; Wong, M. W.; Gonzalez, C.; and Pople, J. A.; *Gaussian 03*, Revision B.03; Gaussian, Inc.: Pittsburgh, PA, 2003.

(34) Zygmunt, S. A.; Mueller, R. M.; Curtiss, L. A.; Iton, L. E. *J. Mol. Struct. (THEOCHEM)* **1998**, *430*, 9−16.

(35) Becke, A. D. *J. Chem. Phys.* **1993**, *98*, 5648−5652.

(36) Sauer, J. *Chem. Rev.* **1989**, *89*, 199−255.

(37) Kramer, G. J.; de Man, A. J. M.; van Santen, R. A. *J. Am. Chem. Soc.* **1991**, *113*, 6435−6441.

(38) Kramer, G. J.; van Santen, R. A.; Emeïs, C. A.; Nowak, A. K. *Nature* **1993**, *363*, 529−531.

(39) Brand, H. V.; Curtiss, L. A.; Iton, L. E. *J. Phys. Chem.* **1992**, *96*, 7725−7732.

(40) Rozanska, X.; van Santen, R. A.; Hutschka, F.; Hafner, J. *J. Am. Chem. Soc.* **2001**, *123*, 7655−7667.

(41) Vollmer, J. M.; Truong T. N. *J. Phys. Chem. B* **2000**, *104*, 6308−6312.

(42) Sierka, M.; Sauer, J. *J. Phys. Chem. B* **2001**, *105*, 1603−1613.

(43) Vos, A. M.; Rozanska, X.; Schoonheydt, R. A.; van Santen, R. A.; Hutschka, F.; Hafner, J. *J. Am. Chem. Soc.* **2001**, *123*, 2799−2809.

(44) Meier, W. M.; Olson, D. H. *Atlas of Zeolite Structure Types*, 2nd rev. ed.; Butterworths: London, 1987.

(45) Sarv, P.; Tuherm, T.; Lippmaa, E.; Keskinen, K.; Root, A. *J. Phys. Chem.* **1995**, *99*, 13763−13768.

(46) Baba, T.; Komatsu, N.; Ono, Y.; Sugisawa, H.; *J. Phys. Chem. B* **1998**, *102*, 804−808.

(47) Ryder, J. A.; Chakraborty, A. K.; Bell, A. T. *J. Phys. Chem. B* **2000**, *104*, 6998−7011.

(48) Franke, M. E.; Sierka, M.; Simon, U.; Sauer, J. *Phys. Chem. Chem. Phys.* **2002**, *4*, 5207−5216.

(49) Fermann, J. T.; Blanco, C.; Auerbach, S. *J. Chem. Phys.* **2000**, *112*, 6779−6786.

(50) Brändle, M.; Sauer, J. *J. Am. Chem. Soc.* **1998**, *120*, 1556−1570.

(51) Lo, C.; Trout, B. L. *J. Catal.* **2004**, *227*, 77−89.

(52) Svelle, S.; Kolboe, S.; Olsbye U.; Swang, O. *J. Phys. Chem. B* **2003**, *107*, 5251−5260.

(53) Blaszkowski, S. R.; van Santen, R. A. *J. Phys. Chem.* **1995**, *99*, 11728−11738.

(54) Sinclair, P. E.; Catlow, C. R. A. *J. Chem. Soc., Faraday Trans.* **1997**, *93*, 333−345.

(55) Zicovich-Wilson, C. M.; Viruela, P.; Corma, A. *J. Phys. Chem.* **1995**, *99*, 13224−13231.

(56) Vos, A. M.; Nulens, K. H. L.; De Proft, F.; Schoonheydt, R. A.; Geerlings, P. *J. Phys. Chem. B* **2002**, *106*, 2026−2034.

(57) Viruela-Martin, P.; Zicovich-Wilson, C. M.; Corma, A. *J. Phys. Chem.* **1993**, *97*, 13713−13719.

(58) Rigby, A. M.; Kramer, G. J.; van Santen, R. A. *J. Catal.* **1997**, *170*, 1−10.

(59) Boronat, M.; Viruela, P.; Corma, A. *J. Phys. Chem. A* **1998**, *102*, 982−989.

(60) Sinclair, P. E.; de Vries, A.; Sherwood, P.; Catlow, C. R. A.; van Santen, R. A. *J. Chem. Soc., Faraday Trans.* **1998**, *94*, 3401−3408.

(61) Senger, S.; Radom, L. *J. Am. Chem. Soc.* **2000**, *122*, 2613−2620.

(62) Svelle, S.; Kolboe, S.; Swang, O. *J. Phys. Chem. B* **2004**, *108*, 2953−2962.